International Journal of Multidisciplinary Research and Publications
ISSN (Online): 2581-6187

A Comparative Investigation on the Confinement of Gallium Arsenide Quantum Dot with Spherical and Cylindrical Shapes

Sozo T. Harry
[1]Department of Physics, Ignatius Ajuru University of Education, Port Harcourt, Rivers State, Nigeria-500001
Email address: sozoharry@yahoo.com, sozo.harry@iaue.edu.ng

Abstract**—** *Quantum dots, the workhorse of nanotechnology has attracted substantial interest for its unusual electrical and optical capabilities, making it a critical factor in the development of innovative technologies such as quantum computing and optoelectronic devices. The characteristics and uses of nanoscale materials are impacted by quantum confinement phenomena. The amount of these confinement effects is governed by the confinement energy. This work dives into the confinement features of gallium arsenide (GaAs) quantum dots, concentrating on the effect of their morphologies within the confinement regime, specifically comparing spherical and cylindrical configurations. Confinement regimes were first established, and corresponding sizes were sampled for both the spherical and cylindrical geometries. Wavelengths were also calculated for both forms. The research incorporates theoretical modelling, simulation, and analysis to draw relevant comparisons between the two forms. It further elucidates how shape impacts the performance of gallium-arsenide quantum dots.*

Keywords**—** *Confinement energy, confinement regime, emission wavelength, cylindrical confining potential, spherical confining potential, Quantum dot.*

I. INTRODUCTION

Quantum dots are semiconductor nanoparticles with dimensions on the order of the de Broglie wavelength of electrons, leading to quantum confinement effects (Brus, 1986, Reed 1993, Shchukin et al., 2009,). The confinement of charge carriers in three dimensions results in discrete electronic energy levels, making quantum dots distinct from bulk materials. In recent time, quantum dots have emerged as pivotal components in the realm of advanced materials, gaining substantial attention due to their exceptional electronic and optical properties (Joglekar *et al.*, 2019; Efros and Brus, 2021). Among the diverse array of quantum dot materials, Gallium Arsenide (GaAs), a group III-V binary semiconductor stands out as a particularly promising semiconductor, owing to its superior characteristics. The unique behaviour of quantum dots arises from quantum confinement effects, where the size and shape of these nanostructures play a pivotal role in dictating their electronic and optical properties (Brus, 1986; Kuno, 2005; Ornes, 2016). Shape, in particular, has been identified as a critical parameter influencing the behavior of quantum dots, with variations such as spherical and cylindrical configurations exhibiting distinct geometric and electronic attributes (Andreev *et al.*, 1999; Billaud and Truong, 2010).

Previous studies have extensively explored different aspects of quantum dots, including their size, composition, and surface properties (Alivisatos,1996; Saito *et al*., 1999; Harry *et al.*, 2023). However, a nuanced comparative analysis specifically focusing on the influence of shape, particularly between spherical and cylindrical configurations of GaAs quantum dots, remains a research gap that this study aims to address. The importance of shape in determining quantum dot properties has been underscored in literature, with research indicating that it significantly affects energy band structures, charge carrier dynamics, and light-emission properties (Lozovskiy and Pyatnytsya, 2011). Consequently, a comprehensive investigation into the confinement effects associated with different shapes is crucial for optimizing the design and performance of GaAs quantum dots.

The versatility of quantum dots makes them invaluable for applications ranging from electronics to photonics and quantum information processing (Kamat, 2013; Nurmikko 2015; Montanarella, and Kovalenko 2022; Deshmukh and Mulay 2023) As such, a deeper understanding of how the shape of GaAs quantum dots impacts their behavior is paramount for harnessing their full potential in the development of cutting-edge technologies (Kongkanand *et al.*, 2008). This study endeavors to bridge existing knowledge gaps by employing theoretical modeling and numerical simulations to conduct a comparative analysis of spherical and cylindrical GaAs quantum dots, shedding light on their distinct confinement characteristics and potential implications for practical applications.

II. SPHERICAL GALLIUM ARSENIDE QUANTUM DOT

A spherical quantum dot is taken into consideration to be a round shaped semiconductor nanocrystal wherein excitons are contained within an endless spherical well. This is equivalent to an impenetrable tough round partitions, hence the infinite barrier approximation. The confining potential is given in Equation 1 as (Delerue and Lannoo, 2004; Harry *et al.*, 2023):

$$V_{Conf.} = V_{conf.}(r) = \begin{cases} 0, & r \leq a \\ \infty, & \text{otherwise} \end{cases} \quad (1)$$

where, r and a are the radii of the confining potential and nanocrystal respectively.

The basic equation governing the physics of excitons (particles or carriers) in nanometric semiconductor confined in a potential is the Schrödinger's time-independent wave equation given as (Aruldhas, 2014):

Sozo T. Harry, "A Comparative Investigation on the Confinement of Gallium Arsenide Quantum Dot with Spherical and Cylindrical Shapes," *International Journal of Multidisciplinary Research and Publications (IJMRAP)*, Volume 7, Issue 2, pp. 126-131, 2024.

$\frac{\hbar^2}{2\mu}\nabla^2\Psi$ (x, y, z) + V Ψ (x, y, z) = $E\Psi(x,y,z)$ (2)

In this case, μ represents the particle's mass, E its strength, and Ψ the particle's associated wave characteristic. and ħ is the reduced Planck's constant.

Given that the capacity of a spherical quantum dot relies on its radius from a fixed point, the round polar coordinate's Laplacian ∇^2 is independent of the angular component and may be found as $\nabla^2 = \frac{1}{r^2}\frac{\partial}{\partial r}\left(r^2\frac{\partial}{\partial r}\right)$ (3)

Putting equations 1 and 2 into equation 3 and multiplying through with $\frac{-2\mu}{\hbar^2}$ gives:

$\frac{1}{r^2}\frac{\partial}{\partial r}\left(r^2\frac{\partial}{\partial r}\right) = \frac{-2\mu}{\hbar^2}E\Psi(x,y,z)$ (4)

Assume Ψ (*x*,,) = R(r)G(θ)Q(∅) ; by the method of separation of variables, solution of equation 4 is stated as:

$\frac{1}{R}\frac{d}{dr}\left(r^2\frac{dR}{dr}\right) + k^2r^2 - l(l+1) = 0$ (5)

where, k is given as:

K = $\frac{\sqrt{2\mu E}}{\hbar}$ (6)

Rewriting Equation 5 as:

$\frac{d^2R}{dr^2} + \frac{2}{r}\frac{dR}{dr} + \left[k^2 - \frac{l(l+1)}{r^2}\right]$ R(r) = 0 (7)

Solution to (6) is the superposition of the spherical Bessel function of order l, j_l(kr) and the spherical Neumann function of order l, n_l(kr) stated as (Boas 2003):

$R_{n,l}$(r) = $C_l j_l$(kr) + $D_l n_l(kr)$ (8)

where C and D are constants.

The finite requirement of the wave function suggests that D need to be equal to zero.

Thus:

$R_{n,l}$(r) = $C_l j_l$(kr) (9)

where C_l is the normalization constant and $R_{n,l}$(r), the eigen function.

The physical description of the system demands that no boundary should exist at r = 0. Hence

$R_{n,l}$(d) = $C_l j_l$(kd) (10)

in which d is the diameter of the field (distance between directly opposite points on the sector).

Also, the endless barrier requires that R(d) = 0. This interprets into :

j_l(kd) = 0 (11)

where (kd) is a zero of the lth order spherical Bessel function.

Graphically, the Bessel function depicts an oscillatory characteristic with a varying amplitude and length. Each one has an endless wide variety of zeros. Unfortunately, those zeros aren't placed at excellent(sensible) factors (like n or nπ).

The boundary circumstance requirement is said as:

K = $\frac{1}{d}X_{n,l}$ (12)

in which $X_{n,l}$ is the nth zero of the lth order spherical Bessel function.

Putting (12) into (6) yields:

$\frac{1}{d^2}X_{n,l}^2 = \frac{2\mu E}{\hbar^2}$ (13)

The allowed energies E_n are then given as :

$E_n = \frac{\hbar^2}{2\mu d^2}X_{n,l}^2$ (14)

The electron confinement power E_{ne} is gotten by setting $\mu = m_e^*$ in (14) as :

$E_{ne} = \frac{\hbar^2}{2m_e^* d^2}X_{n,l}^2$ (15)

in which m_e^* is the effective mass of electron.

Similarly, the hole confinement energy E_{he} is obtained by setting $\mu = m_h^*$ in (15)

$E_{he} = \frac{\hbar^2}{2m_h^* d^2}X_{n,l}^2$ (16)

Here m_h^* is the effective mass of hole.

Adding (15) and (16) offers the confinement energy (genuinely confinement power) E_{conf}^S for the spherical shaped gallium arsenide quantum dot as:

$E_{conf}^S = \frac{\hbar^2}{2d^2}\left(\frac{1}{m_e^*} + \frac{1}{m_h^*}\right)X_{n,l}^2$ (17)

wherein n represents the radial quantum range and l the orbital angular momentum. The floor country corresponds to $n = 1$ and $l = 0$; $X_{1,0}$= 3.142 (Oliver *et al*, 2010).

(17) is restated as

$E_{conf}^S = \frac{\pi^2\hbar^2}{2d^2}\left(\frac{1}{m_e^*} + \frac{1}{m_h^*}\right)$ (18)

III. Cylindrical Gallium Arsenide Quantum Dot

An ideal cylindrical-shaped quantum dot is a cylindrical-shaped semiconductor nanocrystal in which electrons and holes relative to excitons are confined in an infinite cylindrical potential well; the confining potential is given as (Harry et al., 2023): This infinite potential corresponds to impenetrable hard cylindrical walls, sometimes known as the Dirichlet problem for a cylinder.

$V_{conf.}(r) = \begin{cases} 0, & r \le a,\ 0 < z < L \\ \infty, & \text{otherwise} \end{cases}$ (19)

where r and L are the radius and length of the cylinder respectively.

The basic equation governing the physics of carriers in a nanometric sized semiconductor is the Schrodinger time-independent wave equation stated in Equation 2.

Putting (19) into (2) in cylindrical coordinate and multiplying by $\frac{2\mu}{\hbar^2}$ gives

$\left[\frac{1}{r}\frac{\partial}{\partial r}\left(r\frac{\partial\Psi}{\partial r}\right) + \frac{1}{r^2}\frac{\partial^2\Psi}{\partial\emptyset^2} + \frac{\partial^2\Psi}{\partial Z^2}\right] = -\frac{2\mu}{\hbar^2}E\Psi$ (20)

Using the method of separation of variables and assuming the product ansatz:

Ψ(r,Ψ,Z) = R(r) Q(∅) $Z(z)$ (21)

Putting (21) into (2), dividing by RQZ and rearranging gives

Sozo T. Harry, "A Comparative Investigation on the Confinement of Gallium Arsenide Quantum Dot with Spherical and Cylindrical Shapes," *International Journal of Multidisciplinary Research and Publications (IJMRAP)*, Volume 7, Issue 2, pp. 126-131, 2024.

$$\frac{1}{rR(r)}\left(\frac{dR}{dr}+r\frac{d^2R}{dr^2}\right)+\frac{1}{r^2Q(\emptyset)}\frac{d^2Q}{d\emptyset^2}+\frac{1}{Z(z)}\frac{d^2Z}{dz^2}=-\frac{2\mu}{\hbar^2}E \quad (22)$$

Using the following substitutions:

$$\frac{1}{Q}\frac{d^2Q}{d\emptyset^2}=-k_1^2 \;;\quad \frac{1}{Z}\frac{d^2Z}{dz^2}=-k_z^2;\quad \frac{2\mu E}{\hbar^2}=k_3^2;$$

$$k^2=k_3^2-k_z^2 \quad (23)$$

Recall the Z- Equation of (23)

$$\frac{1}{Z}\frac{d^2Z}{dz^2}=-k_z^2$$

Solution to the above considering boundary conditions is given as:

$$Z(z)=Sin\,(k_zZ) \quad (24)$$

where, k_z is the wave vector in the z direction.

The wavefunction must varnish at boundaries, hence $Z(L)=0$. For ground state where n_z =1, this corresponds:

$$k_z\mathrm{L}=\pi \quad (25)$$

Putting (23) into (22) and rearranging yields:

$$\frac{1}{rR(r)}\left(\frac{dR}{dr}+r\frac{d^2R}{dr^2}\right)-\frac{k_1^2}{r^2}+k^2=0 \quad (26)$$

Multiplying (26) by Rr^2 and rearranging yields:

$$r^2\frac{d^2R}{dr^2}+r\frac{dR}{dr}+[(kr)^2-k_1^2]=0 \quad (27)$$

(27) is a Bessel equation and has solution given as:

$$R(r)=Aj_{k_1}(kr)+BN_{k_1}(kr) \quad (28)$$

The fact that wave function must varnish at opposite ends and not at the origin. Hence, putting $r=d(diameter)$ reduces (28) to :

$$R(r)=A_3j_{k_1}(kd) \quad (29)$$

This translate into:

$$j_{k_1}(kd)=0 \quad (30)$$

where (kd) is the root of the Bessel function of order k_1 (for ground state, $k_1=1$).

First zero of Bessel function of order one equals 3.8317 ((Oliver *et al*, 2010).

Putting this into (30) and solving for k yields:

$$k=\frac{3.8317}{d} \quad (31)$$

Using (23) and solving for the energy yields:

$$\mathrm{E}=\frac{\hbar^2k_3^2}{2\mu}=\frac{\hbar^2k^2}{2\mu}+\frac{\hbar^2k_z^2}{2\mu}$$

$$\mathrm{E}=\frac{\hbar^2k^2}{2\mu}+\frac{\hbar^2k_z^2}{2\mu} \quad (32)$$

The electron confinement energy, $\mathrm{E_{ne}}$ is obtained by putting $\mu=m_e^*$ into (32) and is stated as:

$$\mathrm{E_{ne}}=\frac{\hbar^2k^2}{2m_e^*}+\frac{\hbar^2k_z^2}{2m_e^*} \quad (33)$$

where m_e^* is effective mass of electron

Similarly, hole confinement energy $\mathrm{E_{he}}$, is obtained by putting $\mu=m_h^*$ into (32)

$$\mathrm{E_{he}}=\frac{\hbar^2k^2}{2m_h^*}+\frac{\hbar^2k_z^2}{2m_h^*} \quad (34)$$

where m_h^* is effective mass of hole.

Total confinement for the cylindrical shaped gallium arsenide quantum dot $\mathrm{E_{conf}^C}$ is the sigma of the confinement energies due to the electrons and due to the holes. This gives

$$\mathrm{E_{conf}^C}=\frac{\hbar^2(k^2+k_z^2)}{2}\left(\frac{1}{m_e^*}+\frac{1}{m_h^*}\right) \quad (35)$$

Putting (25) and (31) into (35) yields the ground state confinement energy for a cylindrical shaped quantum dot as:

$$\mathrm{E_{conf}^C}=\frac{\hbar^2}{2}\left[\left(\frac{3.8317}{d}\right)^2+\left(\frac{\pi}{L}\right)^2\right]\left(\frac{1}{m_e^*}+\frac{1}{m_h^*}\right) \quad (36)$$

IV. Emission Wavelength and Confinement Energy

From wave mechanics:

$$\lambda_b=\frac{h}{p}, \quad (37)$$

Where λ_b is de Broglie wavelength, and p, momentum of particle.

Energy and momentum are related as (Aruldhas, 2014):

$$E=Pc \quad (38)$$

Where E is energy of particle and c, speed of light

Using (37) and (38), the emission wavelength λ_e is obtained as:

$$\lambda_e=\frac{hc}{\Delta E}, \quad (39)$$

V: Equivalence Between Sphere and Cylinder

Volume of sphere $\mathrm{V_s}=\frac{4}{3}\pi r_s^3$ (40)

where r is the radius and π, a constant.

Volume of cylinder $\mathrm{V_c}=\frac{1}{3}\pi r_c^2\mathrm{L}$ (41)

where r_c is the radius, L is the length and π, a constant.

For equivalence , $\mathrm{V_s}=\mathrm{V_c}$.

In terms of diameter, the equivalence is stated as:

$$\mathrm{L}=2\mathrm{d} \quad (42)$$

Where L is length of cylinder and d, diameter of cylinder.

V. Computation of Confinement Energies of Spherical and Cylindrical Shaped Gallium Arsenide Quantum Dots

(18) was used to compute for the confinement energy $\mathrm{E_{conf}^S}$ of the spherical shape, Equations 36 and 39 were used to compute for the confinement energy $\mathrm{E_{conf}^C}$ of equivalent cylindrical shaped Gallium Arsenide quantum dot respectively within the confinement regime while (30) was used to compute for the emission wavelength for both shapes. In arriving at the results, the following parameters of Gallium Arsenide were used: bulk bandgap (at 300K) $=1.42\ eV$, exciton bohr radius, $\mathrm{a_B}=11.3$ nm, Planck's constant h $=6.63\mathrm{x}10^{-34}\mathrm{Js}$, electron rest mass, $\mathrm{m_0}=9.11\mathrm{x}10^{-21}\mathrm{Kg}$, effective mass of electron $\mathrm{m_e^*}=0.067\ \mathrm{m_0}$, effective mass of hole, $\mathrm{m_h^*}=0.50\ \mathrm{m_0}$, $\pi=3.142$, $\mathrm{c}=3\mathrm{x}10^8ms^{-2}$ (Davies, 2005).

The sampled sizes (diameter) are 2.46, 4.46, 6.46, 8.46, 10.60, 12.46, 14.46, 20.00, 25.00, and 30.00 nm.

Sozo T. Harry, "A Comparative Investigation on the Confinement of Gallium Arsenide Quantum Dot with Spherical and Cylindrical Shapes," *International Journal of Multidisciplinary Research and Publications (IJMRAP)*, Volume 7, Issue 2, pp. 126-131, 2024.

Table 1 showing the computed confinement energies for both spherical and cylindrical Gallium arsenide quantum dots with their corresponding dot sizes (diameters).

TABLE 1: Gallium Arsenide quantum dot with minimum size, $L = 2.37nm$

$m_e^* = 0.067m_0$; $m_h^* = 0.50m_0$;

S/N	Dot diameter(nm)	Confinement energy (eV)	
		Spherical	Cylindrical
1	2.46	1.0542	1.8266
2	4.46	0.3207	0.5561
3	6.46	0.1529	0.2648
4	8.46	0.0892	0.1546
5	10.60	0.0568	0.0985
6	12.46	0.0411	0.0713
7	14.46	0.0306	0.0501
8	20.00	0.0159	0.0277
9	25.00	0.0102	0.0177
10	30.00	0.0710	0.0123

TABLE 2: Computed wavelength and size for Gallium Arsenide quantum dot

S/N	Dot diameter(nm)	Wavelength λ_e (nm)	
		Spherical	Cylindrical
1	2.46	502.4	382.9
2	4.46	714.2	629.1
3	6.46	790.3	637.8
4	8.46	823.7	789.5
5	10.60	841.8	818.7
6	12.46	850.8	833.6
7	14.46	857.0	845.6
8	20.00	865.7	858.7
9	25.00	869.2	864.7
10	30.00	871.1	868.0

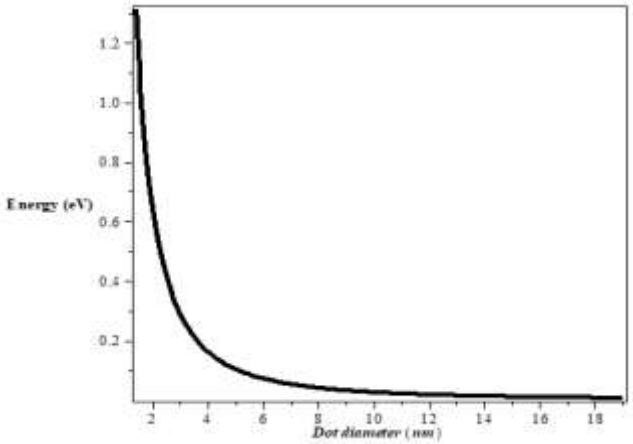

Fig. 1: Ground state confinement energy as a function of diameter for Gallium Arsenide spherical shaped quantum dot

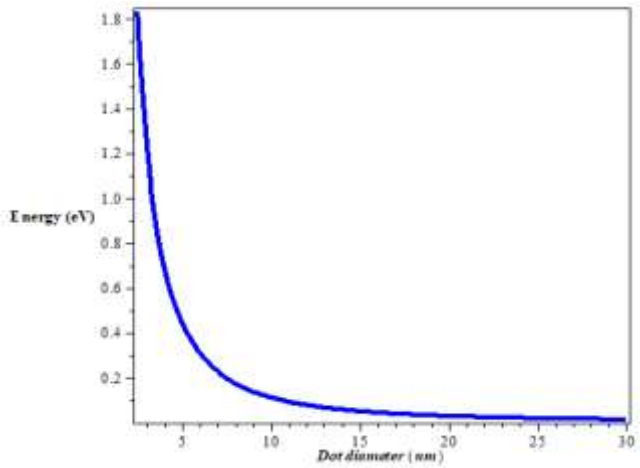

Fig. 2: Ground state confinement energy as a function of diameter for Gallium Arsenide cylindrical shaped quantum dot

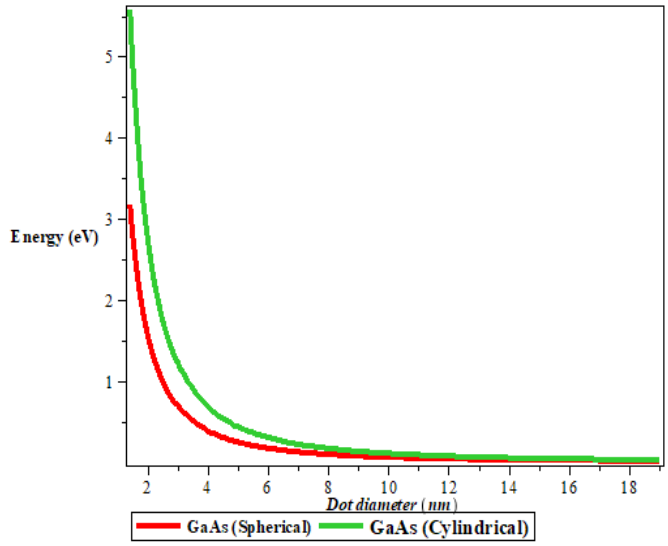

Fig. 3: Combined plot for ground state confinement energy as a function of diameter for spherical and cylindrical shaped Gallium Arsenide quantum dot

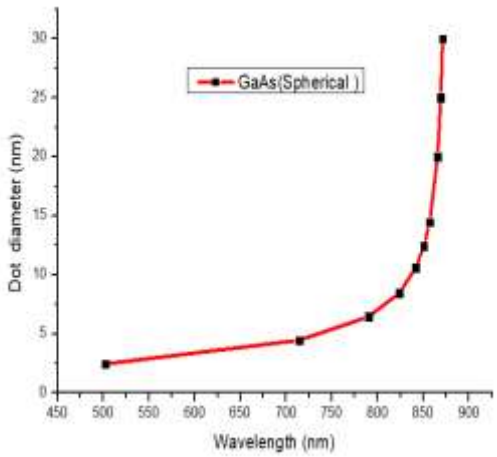

Fig.4: Sizing curve for spherical Gallium Arsenide quantum dot

Sozo T. Harry, "A Comparative Investigation on the Confinement of Gallium Arsenide Quantum Dot with Spherical and Cylindrical Shapes," *International Journal of Multidisciplinary Research and Publications (IJMRAP)*, Volume 7, Issue 2, pp. 126-131, 2024.

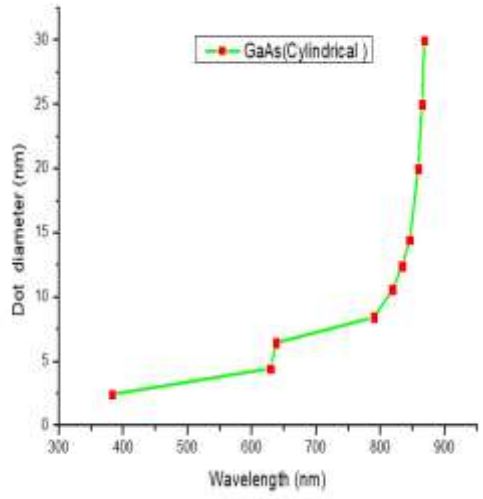

Fig. 5: Sizing curve for cylindrical Gallium Arsenide quantum dot

VI. Discussion of Results

The graphs of ground state confinement energy against size (diameter) for each spherical and cylindrical Gallium Arsenide (GaAs) quantum dots in Figures 1 and 2 depict the dependence of confinement power on the dimensions of quantum dots. The result shows that ground state confinement energy is inversely proportional to the diameter of quantum dot for each shapes Figures 1 and 2 depict two graphs that are asymptotically related to the horizontal axis, or diameter. Therefore, the confinement power drops but never reaches zero as the diameter increases. That is to say, a spherical or cylindrical Gallium Arsenide quantum dot lowest energy isn't always zero.

The confinement energy in a quantum dot is found by increasing the strength of the band gap. Confinement begins when the size (or diameter) of the quantum dot pattern is similar to or of the order of the exciton bohr radius a_B (10 nm for Gallium Arsenide). To put it another way, when the dimensions are similar to 2a_B (doubles the exciton bohr radius). Alternatively, one may want to say that confinement begins when the scale or diameter of the quantum dot sample is comparable to the de Broglie wavelength of the provider (electrons and holes). The power of confinement increases as the quantum dot's dimensions are gradually reduced until the minimal size (the magic and cluster length restrict) is reached, which is set 2.37 nm. nm nm for Gallium Arsenide.

At this limit, the crystal losses its stability (Brus, 1984). Figure 3 shows that in general, confinement is stronger in cylindrical Gallium Arsenide than in spherical Gallium Arsenide quantum dot.

Figures 4 shows the sizing curve (graph of size against wavelength) for spherical shaped Gallium arsenide quantum dot. Also, Figure 5 shows the sizing curve for equivalent sizes of cylindrical Gallium Arsenide quantum dot. The graphs show the same pattern within the confinement regime for the different shapes. The both shapes exhibit an exponential dependence on size of quantum dot. Thus, irrespective of shape, one can conclude that the larger the dot, the redder (lower energy) its fluorescence spectrum would be. Conversely, smaller quantum dots emit bluer (higher energy) light. The coloration is explicitly related to the energy levels of the quantum dot. The vast application of quantum dots is emission based and depends on the sizing curves. The visible portion of the electromagnetic spectrum which spans from about 400 nm to 700 nm is that region of wavelength that is detectable by the human eye. Table 2 shows that emission wavelength of Gallium Arsenide spans through the visible spectrum irrespective of the shape. This partly explains why Gallium Arsenide quantum dots are used in applications such as light emitting diodes, laser diodes, etc.

References

[1] A. P. Alivisatos. Semiconductor clusters, nanocrystals, and quantum dots, *Science*, vol. 271, issue 5251, pp. 933 – 937, 1996.
[2] A. D. Andreev, J. R. Downes, D.A. Faux, and E.P. O'Reily, Strain distributions in quantum dots of arbitrary shape, *Journal of Applied Physics*, vol. 86, issue 1, pp. 297 – 305, 1999.
[3] G. Aruldhas, *Quantum Mechanics.* PHI Learning Private Limited. pp. 42 -43, 2014.
[4] B.Billaud, and T. Truong, (2010). Some theoretical results in semiconductor spherical quantum dots. *Computational material science.* vol. 49, issue 4, pp. S322-S325, 2010.
[5] M. L .Boas, (2005). *Mathematical Methods in the Physical sciences*. John Wiley & sons. Pp. 611 - 615, 2005.
[6] L.E. Brus, Electron–electron and electron-hole interactions in small semiconductor crystallites: the size dependence of the lowest excited electronic state. *The Journal of Chemical Physics.* vol. 80 issue 9, pp. 4403-4409, 1984.
[7] L.E. Brus "Electronic Wave Functions in Semiconductor Clusters: Experiment and Theory." *The Journal of Physical Chemistry*, vol. 90, issue 12, pp. 2555 – 2560, 1986.
[8] J.H. Davies, *The Physics of low-Dimensional Semiconductors: An Introduction*, 6th Reprint Edition, Cambridge University Press, New York, pp. 428 – 431, 2005.
[9] Delerue, and M. Lannoo. *Nanostructures: Theory and Modelling*. Springer. Pp. 47 – 54, 2004
[10] S. Deshmukh and P. Mulay, A drop of quantum dots in the ocean of quantum computing. *Collnet Journal of Scientometrics and Information Management*. vol. 17, issue 1, pp. 141-157, 2023.
[11] A.L Efros, and L.E. Brus, Nanocrystal quantum dots: From discovery to modern development, *ACS Nano.* Vol. 15, issue 4, pp. 6192 – 6210, 2021.
[12] V.A Shchukin, N.N. Ledentsov, and D. Bimberg,. *Epitaxy of Nanostructures*. Springer-Verlag, 387p. 2009.
[13] S, T. Harry, A. D. Antia, and I. B. Okon, Simulation of size for quantum confinement effects in Cadmium selenide quantum dot. *International Research Journal of Modernization in Engineering, Technology and science*. Vol. 5, issue 12, pp. 3808 – 3815, 2023.
[14] P. Joglekar, D. Mandalkar, M. Nikam, N. Pande, and A. Dubal. Review article on quantum dots: synthesis, properties and application. *International Journal of Research in Advent Technology* vol. 7, issue 1, pp. 510 – 515, 2019.
[15] P. Kamat. Quantum dot solar cells: The next big thing in photovoltaics. *Journal of Physical Chemistry Letters*, vol. 4, issue 6, pp. 908 – 913, 2013.
[16] A. Kongkanand, K. Tvrdy, K. Takechi, M. Kuno, and P. V. Kamat, Quantum dot solar cells. Tuning photoresponse through size and shape control of CdSe −TiO2 architecture. *Journal of the American Chemical Society*, vol. 130, issue 12, pp. 4007 – 4015, 2008.
[17] M. Kuno. *Introduction to Nanoscience and Nanotechnology*: A Workbook. CreateSpace Publishing Platform, pp. 37 – 55, 2005.
[18] V. Lozovskiy, and V. Pyatnytsya, The analytical study of electronic and optical properties of pyramid -like and cone-like quantum dots. *Journal of Computational and Theoretical Nanoscience* vol. 8, pp. 1 – 9, 2011.
[19] F. Montanarella,. and M. V. Kovalenko. (2022). Three Millennia of Nanocrystals. *ACS Nano* vol. 16, issue 4, pp. 5085-5102, 2022.

[20] A. Nurmikko. What future for quantum dot-based light emitters? *Nature Physics.* vol. 10, issue 12, pp. 1001 – 1004, 2015.
[21] S. Ornes, (2016). *Quantum dots*. *Proceedings of the National Academy of Sciences*, vol. 113, issue 11, pp. 796 – 2797, 2016.
[22] F. W. Oliver, D. W. Lozier, R. F. Biosvert, and C. W. Clark. NIST Handbook of mathematical fuctions. Cambridge university press, New York, pp.234 – 235, 2010.
[23] M. Reed. Quantum dots. *scientific American*, vol. 268, issue 1, pp. 118-123. 1993.
[24] O. K. Saito, K. Nishi, and S. Sugou.. Shape transition of InAs quantum dots by growth at high temperature. *Applied Physics Letter*, vol. 74, issue 9, pp. 1224 – 1226, 1999.